EIGHTH EUROPEAN ROTORCRAFT FORUM

Paper No. 2.5

AN INVESTIGATION OF THE AERODYNAMICS OF AN RAE SWEPT TIP USING A MODEL ROTOR

by

P.G. Wilby (RAE)

J.J. Philippe (ONERA)

August 31 to September 3, 1982

AIX-EN-PROVENCE, FRANCE

Association Aeronautique et Astronautique de France

AN INVESTIGATION OF THE AERODYNAMICS OF AN RAE SWEPT TIP USING A MODEL ROTOR

by

P.G. Wilby (RAE) and J.J. Philippe (ONERA)

1 INTRODUCTION

The interest at the RAE in swept tips for helicopter rotor blades started in 1972 following the work of Caradonna[1] on a method for predicting the pressure distribution over a blade tip in supercritical flow. At the RAE, Grant[2] began to develop a similar method which was valid for general planform shapes and a range of azimuth angles. Although time dependent methods appeared elsewhere, the RAE method did not include the time dependent terms because of the associated large increase in computing time. At ONERA, an interest in blade tip aerodynamics also began about 10 years ago and led to experimental investigations of pressure distributions on non-lifting rotors with both straight and swept tips[3,4]. These fundamental studies have resulted in the design by ONERA of a sweptback parabolic tip[5].

In parallel with these activities, the techniques for detailed pressure plotting of rotor blades in flight were being developed at the RAE. With this common interest and the complementary activities in mind, a collaborative programme of work was set up between France and the UK which was to involve model rotor tests at ONERA on a swept tip of RAE design and flight experiments at the RAE, using a Puma helicopter, with a further tip design. The two tip planforms are shown in Fig 1. For the Puma blade tip it was essential to keep the centre of pressure on the torsional axis of the blade, which accounts for the leading-edge extension, but this was not necessary for the very stiff model rotor blades. The flight tests with the Puma are just beginning and it is hoped to report on that work at next years Forum. This paper will describe the model rotor tests carried out in the ONERA S2 wind-tunnel at Chalais Meudon.

2 BLADE DESIGN

In order to obtain a comparison between swept and straight blade tips, it was decided to base the blade design on the blades of a model rotor that had been tested previously at ONERA[5]. The blade design for this latter rotor is shown in Fig 2 and was of low aspect ratio (R/c = 7) to allow the installation of chordwise arrays of pressure transducers. The blade section was cambered with a thickness-to-chord ratio of 0.12 out to 70%R, from where the thickness reduced to 0.06c at the tip. A linear twist of 12° was incorporated, and with its three blades the rotor had a solidity of 0.137. The new blades with their swept tips were to retain the same overall dimensions, section, thickness taper and twist as the straight blades.

The design of the swept tip planform was quite straightforward, as shown in Fig 3, with the first step being to give a 30° sweep back to both leading and trailing-edges over about one chordlength of the blade. A rounding-off of the corners was then introduced, as recommended in Ref 2, to give a smoother spanwise variation of pressure distributions and to eliminate a suction peak near the tip extremity. As pressure had been measured at 85%, 90% and 95% rotor radius on the straight blades, pressure transducers were to be located at the same spanwise locations on the swept tips. It will be noted that the change in planform starts at about 0.85R.

Having defined the geometry of the new swept tip, the method for predicting pressure distributions in quasi-steady conditions[2] was used to produce the results shown in Figs 4 and 5 for both tip shapes at zero lift. Fig 4 gives chordwise pressure distributions at 85%, 90% and 95% rotor radius for 90° azimuth at an advance ratio of 0.43. The results indicate that the supercritical flow over the upper surface of the straight blade tip has been effectively eliminated by the swept tip. Fig 5 gives the predicted variation of the pressure distribution at 0.9R over the azimuth range of 60° to 120°, and once more the swept tip is seen to eliminate supercritical flow on the upper surface. There is in all cases a supercritical suction peak at the leading-edge on the lower surface due to the profile camber, but the magnitude of the peak is reduced by the effects of sweepback. The main aim of the model rotor experiment was to determine whether or not these predicted effects of sweepback were to be realized in practice.

3 MODEL TESTS

Pressure transducers were installed in the tips in the way described in Ref 5. Each blade held 1/3 of the total number of transducers for each spanwise station, thus measurements from all the blades were required to complete one chordwise pressure distribution. All the transducers were vented to upper and lower surface holes, and two runs were required (with lower and then upper surface holes sealed) to give upper and lower surface distributions. The blades were built to have detachable tips, with electrical leads contained within the basic blades. Due to an accident in a previous experiment one of the basic blades was damaged and had to be replaced in the swept tip experiment by a blade without electrical connections. This of course meant that the transducers on that blade tip could not be used. Three of the transducers on the other two blades developed faults and could not be used to give reliable results. The final array of usable transducers is given in Table 1. As will be seen, this array was still sufficient to demonstrate the difference between swept and straight tips.

Table 1

Pressure transducer locations

0.85R	0.90R	0.95R
2.8%c	5.4%c	2.9%c
5.2	10.2	5.1
17.2	20.4	16.7
20.2	25.2	20.1
60.2	35.5	30.4
	40.2	35.2
	60.5	50.2
	75.0	75.4

The rotor was mounted in the wind-tunnel, in an inverted position, from the roof of the tunnel as indicated in Ref 5. Only a collective pitch control was available and the tip path plane was controlled by the shaft tilt. The latter was adjusted to give a horizontal component of force equal to the drag force that would be experienced with a fuselage of given equivalent flat plate

area, this being set at 1/10 of the total blade area (which is typical of many helicopters). The tip speed was kept constant at 210 m/s. Tests were carried out on both swept and straight blades over a range of forward speeds bvetween 70 and 90 m/s approximately, with additional tests on the swept tip rotor at 97 m/s. At 90 m/s the advance ratio was 0.43. Measurements were taken at three values of thrust coefficient. Apart from recording the transducer signals, measurements were made of the overall rotor forces and moments, rotor power and the blade flapping angle.

During each test, signals from the pressure transducers could be monitored on a CRT display as a check on any malfunctions. Examples of the traces for 4 transducers at 3 values of forward speed are shown in Fig 6, and these give a clear indication of the presence of supercritical flow on the advancing blade. The strong discontinuities are a result of the shock wave passing across the pressure hole. Smaller disturbances can be seen at 0° azimuth due to the wake from the hub.

Apart from the main interest in the measurement of aerodynamic characteristics of blade tips in this experiment, there was the additional interest in noise. Other researchers have identified a source of noise due to the presence of local supersonic flow over the surface of the blade tips, thus any change in tip shape that affects supercritical flow should also affect noise. With this in mind, three microphones were mounted on the tunnel walls in the positions shown in Fig 7. All three microphones recorded a consistent drop in noise of about 2 dB for the swept tips. However, no further analysis of the noise measurements has been undertaken for this paper.

4 EXPERIMENTAL RESULTS

One of the anticipated benefits of a swept tip is a reduction in profile power at high advance ratio due to the delay in the development of supercritical flow, with its attendant rise in drag, on the advancing blade. Fig 8 shows the measured variation of power coefficient with forward speed for the three values of thrust coefficient. It is seen that the power required is the same for both blade tip shapes at the lower values of forward speed, but power increases less rapidly with speed for the swept tip. For the intermediate value of thrust coefficient, the reduction in power due to the swept tip is 5% at V = 90 m/s. The percentage reduction in profile power will of course be much larger, as the parasite power is significant at high forward speed (it amounts to at least 1/3 of the total power). However, one might argue that due to the low aspect ratio of the blades, the swept tip covers a larger percentage of the rotor radius than would be the case for the average full scale rotor. Thus the power reduction in full scale might be expected to be somewhat less. On the other hand, helicopters with low aspect ratio blades do exist.

An overall picture of the effect of the swept tip on the development of supercritical flow is provided by Fig 9. The upper part shows the azimuthal variation of maximum local Mach number on the upper surfaces of the straight and swept tips at the three radial stations. This gives a measure of the strength of the shock wave that terminates the supercritical region and has a major influence on the magnitude of the drag rise. Maximum local Mach number is seen to be appreciably lower for the swept tip at 0.85R and 0.9R for the whole azimuth sector in which supercritical flow is present. However, at 0.95R shock strength appears to be the same for both tips for azimuth angles greater than 130°. For angles less than 130° there is of course a significant benefit from the swept tip. Apart from shock strength, the other important factor that

affects the level of drag is shock position. The further aft the shock wave sits, the higher will be the drag because of the greater extent of rearward facing surface that is exposed to the low static pressure found ahead of the shock. The lower part of Fig 9 is thus of interest as it shows the chordwise extent of the supercritical flow, from the sonic point near the leading-edge to the shock position further aft. Again, the swept tip shows a clear advantage except over the front of the rotor disc at 0.85R and 0.9R, and for azimuth angles greater than 100° at 0.95R where the shock moves further aft on the swept tip. Fig 10 shows a similar comparison between swept and straight tips at the higher forward speed of 91 m/s. The combined effect of a lower shock strength and further forward shock position for the swept tip over the major portion of the supercritical flow sector can be expected to lead to a significant reduction in profile power, and hence total power, as was seen in Fig 8.

The fact that, over the front of the disc, the shock wave over the outer part of the tip is found to sit further aft on the swept tip is an interesting feature. A possible explanation for this is that in this region of the disc the Mach number of the flow normal to the blade leading-edge is actually greater for the swept tip. This is illustrated in Fig 11 which gives the azimuthal variation of Mach number normal to the leading-edge at 0.925R for both straight and swept tips. At this spanwise station the angle of sweepback is 30° for the swept tip, and even at ψ = 180° the flow normal to the swept leading-edge has contributions from both the rotational and forward speeds of the rotor. In two dimensions it is well known that the shock will move further aft as free-stream Mach number increases.

Having noted these overall comparisons in the supercritical flow regions it is now interesting to examine the greater detail given by the pressure distributions, examples of which are given in Fig 12. Here, pressure distributions are compared for the two tips at 0.85R, 0.9R and 0.95R for azimuth angles of 90°, 120°, 150° and 180°. At ψ = 90° it is clearly seen that the swept tip decreases the strength of the shock wave and moves the shock further forwards. However, at ψ =120°, pressure distributions are almost identical for the two tip shapes at 0.95R. For ψ = 150° and 180° the shock over the outer part of the blade is clearly further aft on the swept tip, but at ψ = 180° it is impossible to be certain of the minimum pressure on the straight tip because of the absence of pressure sensors close to the leading-edge.

The way in which pressure distributions at ψ = 90° change with forward speed is shown in Fig 13 which gives measurements at 0.9R and 0.95R for both tip shapes. It is interesting to note that the shock strength on the swept tip at 97 m/s is still not as great as on the straight tip at 69 m/s. A comparison of straight and swept tip characteristics for the retreating blade could have been of interest but its value is diminished by two features of the rotor. Firstly, there were insufficient pressure sensors close to the leading-edge for an accurate definition of the suction peak to be given at high incidence. Secondly, due to the blade dynamic characteristics, the high incidences usually associated with the retreating side of the rotor disc were not attained in this particular test. The latter fact is demonstrated by Fig 14 which gives the variation of normal force coefficient, C_N , with azimuth at 0.9R for the rotor with the straight tips. The main unusual features are the very low values of C_N , over the rear and retreating sectors of the disc, and the rapid rate of increase of C_N with azimuth at ψ = 90°. The reason for this behaviour is the high moment of inertia of the blades about the flapping hinge, due to the high blade mass, as demonstrated in Fig 15. This figure shows the predicted variation of lift coefficient with Mach number for two values of flapping moment

of inertia. These values are based on an assumption of a uniform distribution of blade mass per unit span, with blade total masses of 1.26 kg (the actual mass of the blades) and 0.25 kg. The high mass blade produces the type of C_L variation found in the present experiment, whilst the low mass blade results in the more usual "figure of eight" variation. A high blade mass was the result of designing for a very stiff blade to avoid aeroelastic deformation, and the incorporation of a metal chassis on which were mounted the pressure transducers. With very high blade mass, flapping relative to the rotor shaft will be suppressed and the rotor becomes more like a propeller, with little compensation for variations in blade lift. Stong rolling moments can therefore be expected. Fig 16 shows that if cyclic pitch could be introduced to trim the rotor with the heavy blades, a more usual form of C_L variation should be achieved.

It should be pointed out that the calculations of C_L variation shown in Figs 15 and 16 were not an attempt to provide an accurate representation of the measured variation, but rather to identify trends. The RAE/WHL rotor performance programme was used, with Glauert downwash distribution and blade section characteristics that are similar to, but not the same as, for the model blade profile. The calculated results are simply to show the effect of high blade mass on the azimuthal variation of C_L .

5 COMPARISONS BETWEEN THEORY AND EXPERIMENT

Having obtained measured pressure distributions on the blade tips it is of interest to see how well these distributions agree with the prediction method that was used to aid the design of the swept tips. However, for several reasons, this is not a straightforward matter. First of all, the prediction method does not allow for unsteady effects or boundary-layers. Secondly, although the prediction method will provide results for a lifting case, a spanwise distribution of incidence must be provided and there is no means of knowing what this is in the experiment. Nevertheless there are some instructive comparisons that can be made.

The first comparison is shown in Fig 17 which gives measured pressure distributions on both swept and straight tips at $\psi = 60°$ on the left, and the equivalent theoretical results on the right. At $\psi = 60°$ the lift on the blade is close to zero, therefore the theoretical results were obtained by assuming that blade incidence was everywhere the zero lift angle for the blade section. Although Fig 17 does not give a direct comparison of theory and experiment, it shows the relative differences between swept and straight tips as given by both experiment and theory. These relative differences are seen to show the same features in experiment and theory. The lower values of upper surface pressure on the straight tip are clearly seen in both cases, with a shock wave terminating a supercritical region at 0.95R. Also, the higher suction peak near the lower surface leading-edge of the straight tip is clearly seen in both experiment and theory at 0.9R - the peak being insufficiently well defined due to the lack of sensors in the experiment at 0.85R and 0.9R. Clearly, the effects of sweepback predicted by theory have been realised in practice.

A direct comparison between theory and experiment for the swept tip is attempted in Fig 18 for $\psi = 90°$. In this case, the spanwise distribution of incidence used in the calculation was adjusted until the predicted distribution of C_L agreed with the measured quantity. The latter was however difficult to determine accurately because of the sparsity of pressure sensors. Distinct differences between theory and experiment are apparent, in particular the higher peak suction of the lower surface for the experimental results, and the lower

pressures between 10% and 30% chord on the upper surface in experiment. In general, these differences are likely to be due to the absence of unsteady effects in the theoretical results. At ONERA a time-dependent three-dimensional prediction method has been developed recently and it is hoped that a comparison between this new method and experiment, for the straight tip, will be included in Ref 6.

Some assessment of the magnitude of unsteady effects at $\psi = 90°$ can be obtained using the two-dimensional time-dependent method of Ref 7 to represent conditions on the straight tip, provided that the variation of incidence with azimuth can be modelled reasonably well. A modelling of the incidence variation has been attempted through a trial and error process in which the prediction method was run assuming a sinusoidal variation of both Mach number and incidence, but allowing some phase difference between the two variables. The best match of predicted and measured variation of C_L with Mach number is shown in Fig 19. As the match is quite good for the azimuth range below $\psi = 90°$ it is felt that the theoretical model provides a satisfactory basis for comparing predicted and measured pressure distributions at $\psi = 90°$. The fact that the measured and modelled variations of C_L with M differ for $90° < \psi < 270°$ is not likely to cause significant errors in the pressure distribution at $\psi = 90°$. The theoretical pressure distribution obtained in this way is compared with the measured distribution in Fig 20, where the main differences are seen to lie in the shock position and in the lift generated over the centre portion of the chord. It must however be remembered that the prediction method does not include viscous effects. Also shown in Fig 20 is the predicted pressure distribution for steady conditions, taking the values of Mach number and incidence that correspond to $\psi = 90°$ in the unsteady calculation. The unsteady effects are clearly quite large.

6 CONCLUSIONS

This experimental investigation was set up to check whether or not the predicted benefits of tip sweepback are realised in practice for the advancing blade. The main conclusion, based on the measurements of power and pressure distributions, is that the benefits are indeed genuine, even though the prediction method neglected time-dependent effects. The onset and development of supercritical flow over the advancing tip is delayed appreciably by the incorporation of tip sweepback.

At the same time, it has been shown that a swept tip increases the effective tip Mach number over the front of the rotor disc and conditions here must be taken into account when designing a swept tip - especially if blade incidence is expected to be high enough in this region to produce supercritical flow. However, it must be pointed out that the power measurements show that any disadvantage over the front of the disc is greatly outweighed by the benefits on the advancing blade, and a significant reduction in overall power is achieved.

Some simple noise measurements suggest that the swept tips may produce a reduction in noise in forward flight.

A strong time-dependent effect has once more been demonstrated on the advancing sector of the disc, showing the need for time-dependent three-dimensional prediction methods.

The limitations of a model rotor having heavy blades and no cyclic pitch have been identified in terms of its ability to reproduce the operating

conditions of a full scale rotor blade tip over the complete azimuth cycle. However, such a model can still provide valuable data on the effect of tip sweep over the advancing and forward sectors of the disc and has thereby fulfilled its original purpose.

An area of great interest that remains to be investigated is the behaviour of a swept tip on the retreating blade, especially in relation to stall onset and post-stall characteristics. It is hoped that the Puma flight experiments at the RAE will provide valuable insight into this topic.

REFERENCES

1. W.F. Ballhaus and F.X. Caradonna. The effect of planform shape on the transonic flow past rotor tips. AGARD Conference Proceedings No. 111, Aerodynamics of Rotary Wings, 1972.

2. J. Grant. The prediction of supercritical pressure distributions on blade tips of arbitrary shape over a range of advancing blade azimuth angles. Vertica, Vol 3, pp 275 to 292, 1979.

3. F.X. Caradonna and J.J. Philippe. The flow over a helicopter blade tip in the transonic regime. Vertica, Vol 2, No.1, 1978.

4. B. Monnerie and J.J. Philippe. Aerodynamic problems of helicopter blade tips. Vertica, Vol 2, pp 217 to 231, 1978.

5. J.J. Philippe and J.J. Chattot. Experimental and theoretical studies on helicopter blade tips at ONERA. Proceedings of the 6th European Rotorcraft and Powered Lift Aircraft Forum, Bristol, September 1980, ONERA TP No. 1980-96.

6. F.X. Caradonna, C. Tung and A. Desopper. Blade vortex flow by finite difference methods. 8th European Rotorcraft Forum, Aix-en-Provence, September 1982.

7. J. Grant. A method for computing steady or time dependent two-dimensional supercritical flow about an aerofoil with application to a helicopter rotor blade. RAE Technical Report 79084, July 1979.

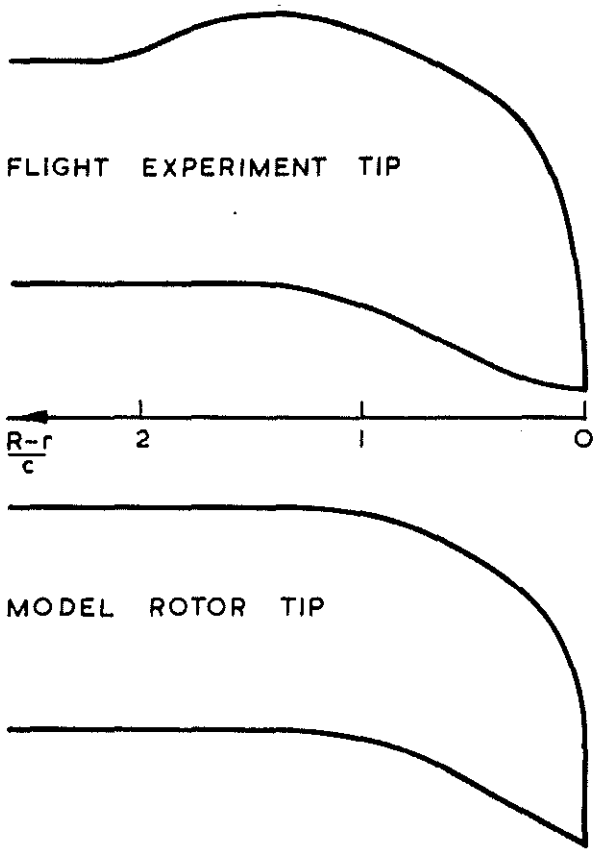

Fig 1 Planforms for swept tip research

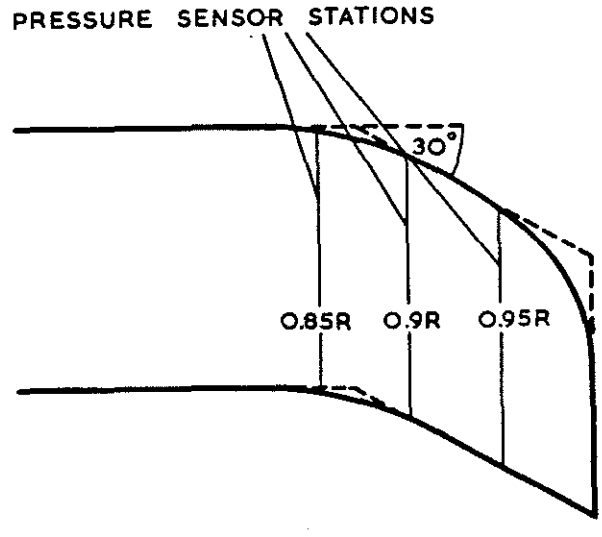

Fig 3 Model swept tip

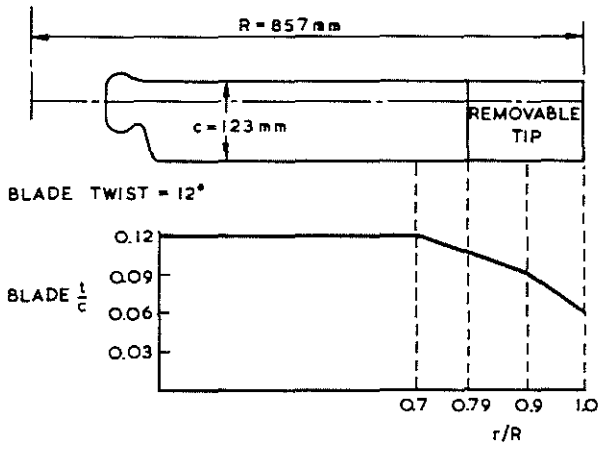

Fig 2 Geometry of reference blade

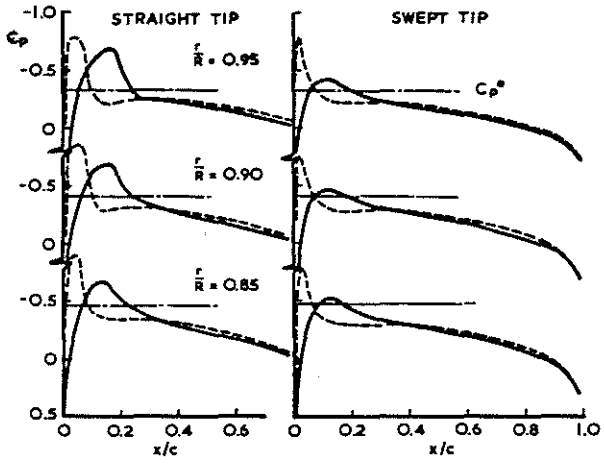

Fig 4 Predicted pressure distributions at zero lift, $\psi = 90^{o}$

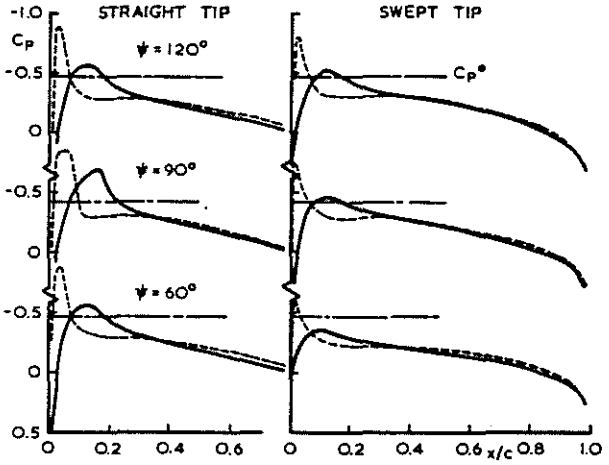

Fig 5 Predicted pressure distributions at zero lift, r = 0.9R

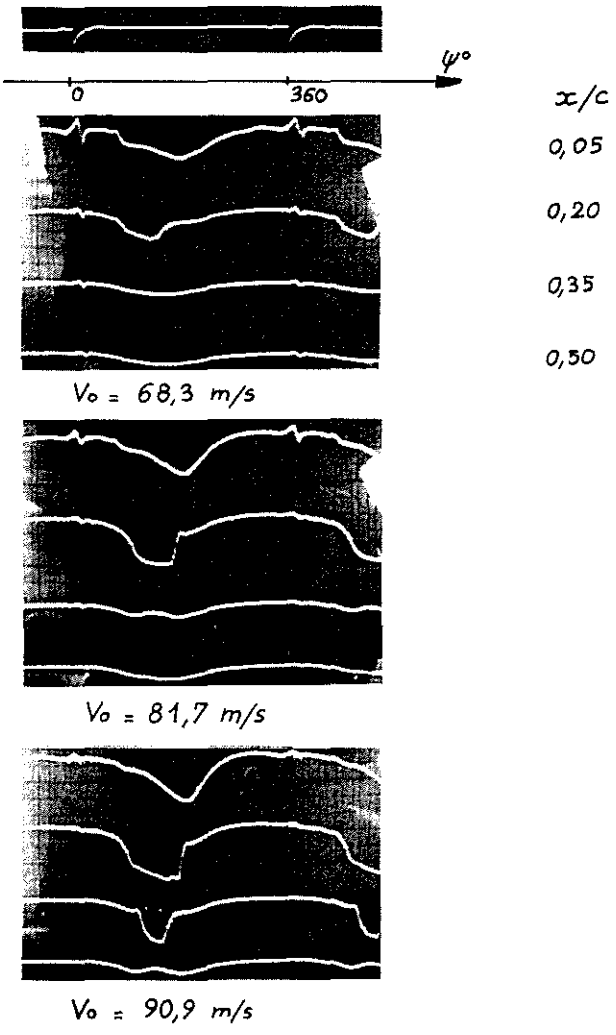

Fig 6 CRT display of pressure sensor signals for straight tip. C_T/σ = 0.0665, r/R = 0.95

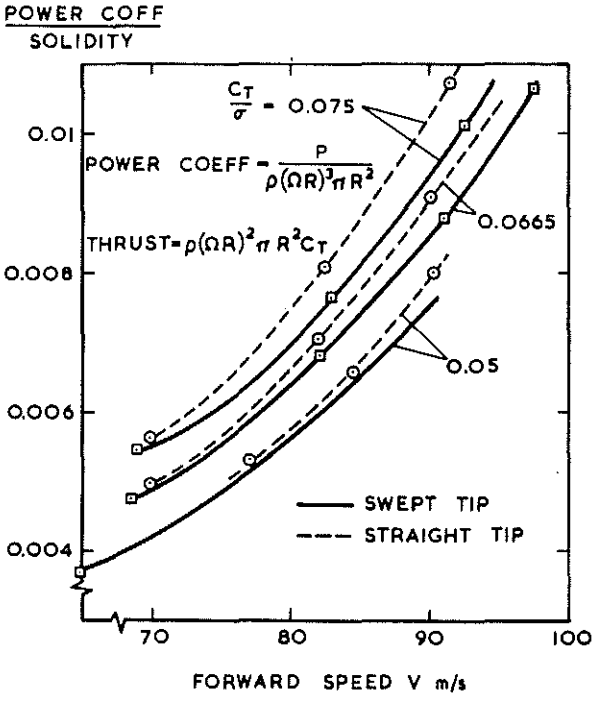

Fig 8 Measured effect of tip shape on power required

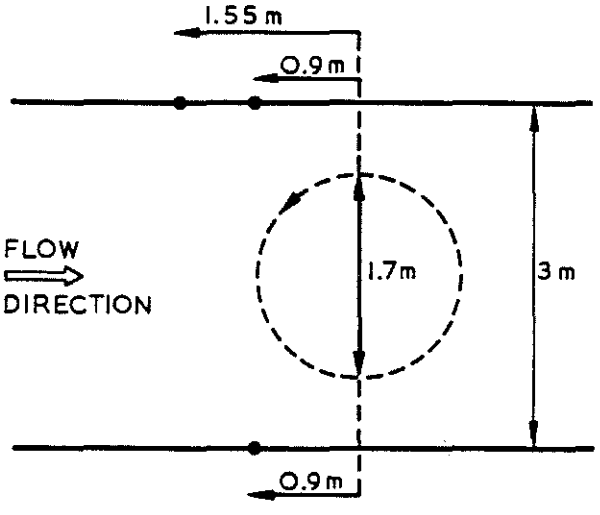

Fig 7 Microphone positions in tunnel walls

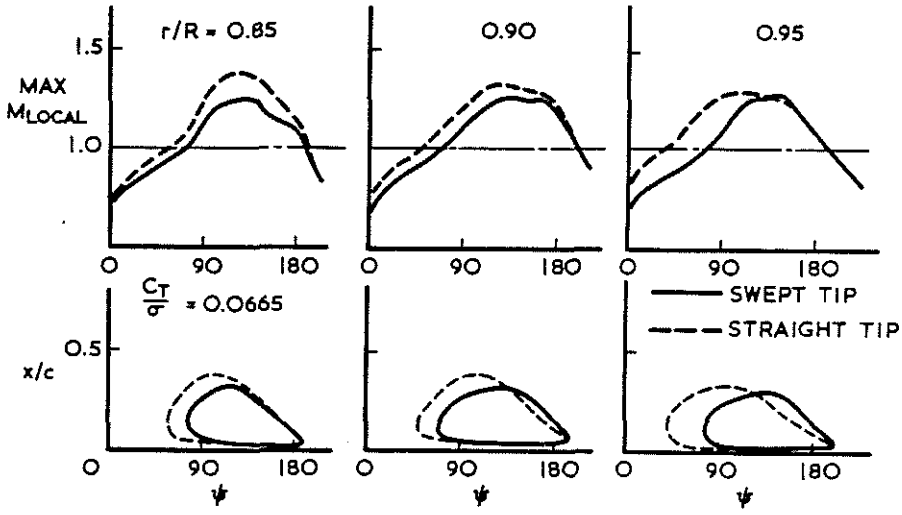

Fig 9 Azimuthal variation of maximum local Mach number and chordwise extent of supercritical flow at V = 82 m/s

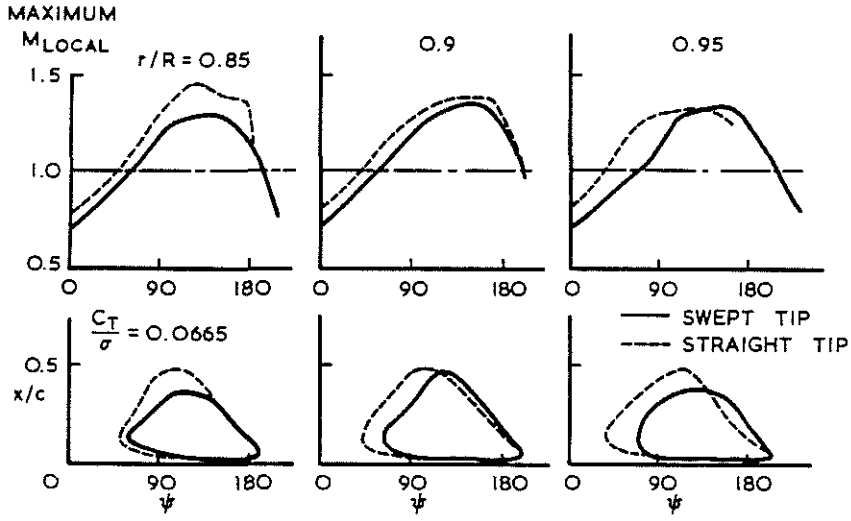

Fig 10 Azimuthal variation of maximum local Mach number and chordwise extent of supercritical flow at V = 91 m/s

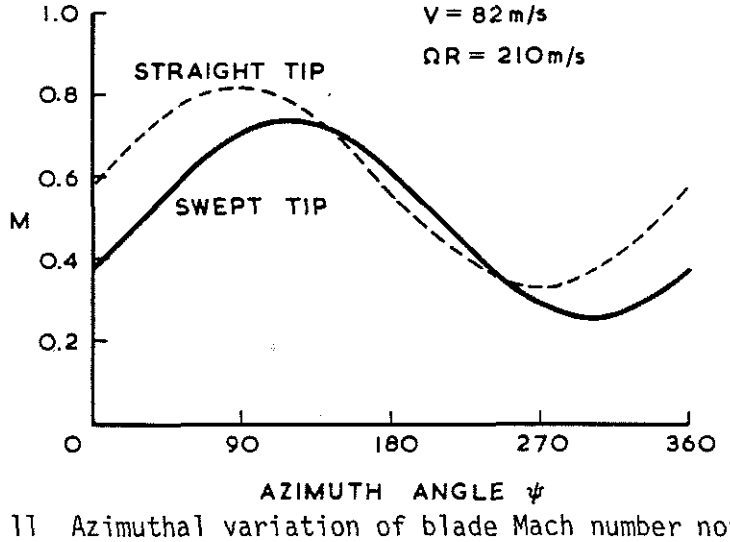

Fig 11 Azimuthal variation of blade Mach number normal to leading-edge at 0.925R

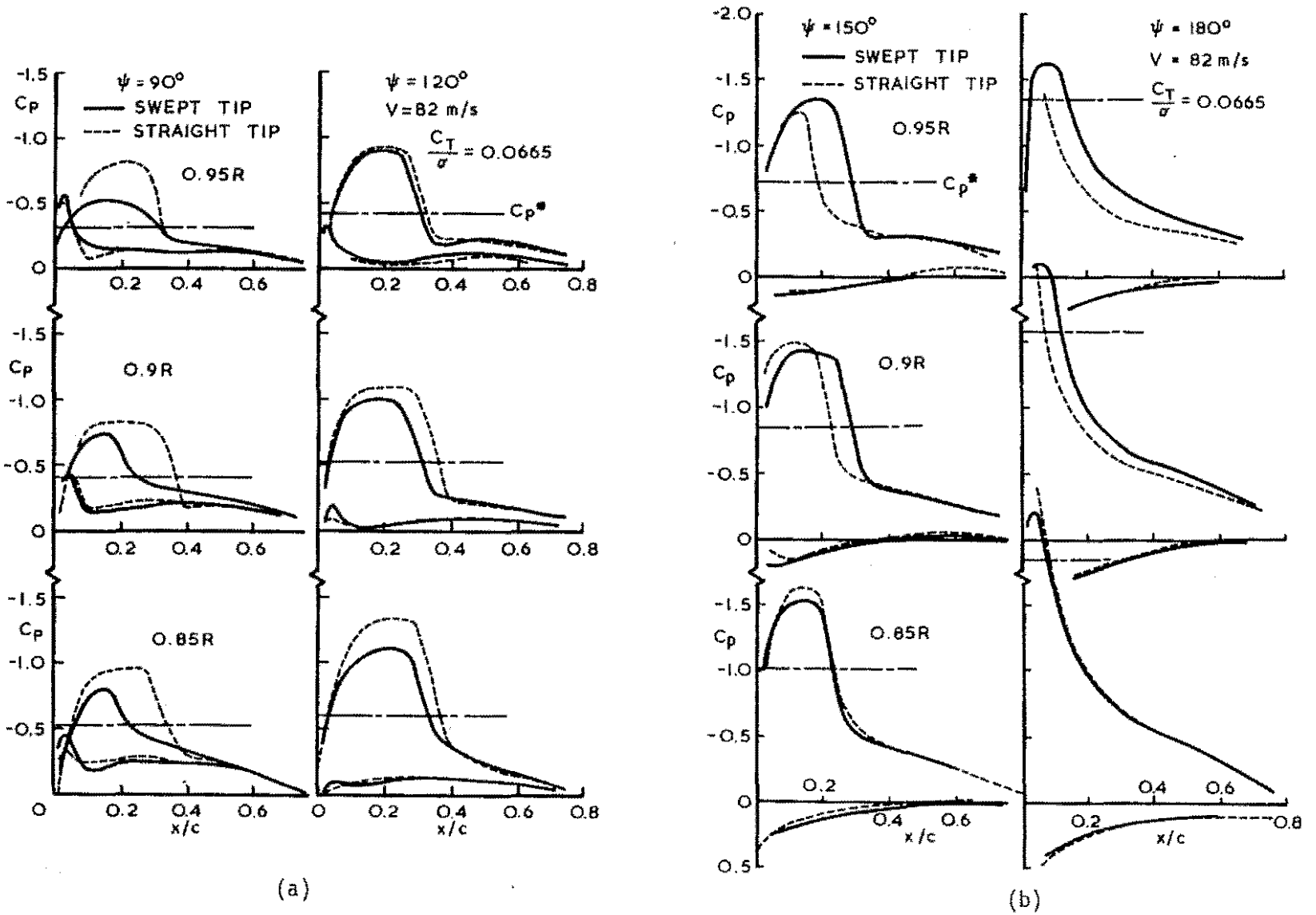

Fig 12a&b Measured pressure distributions for swept and straight tips

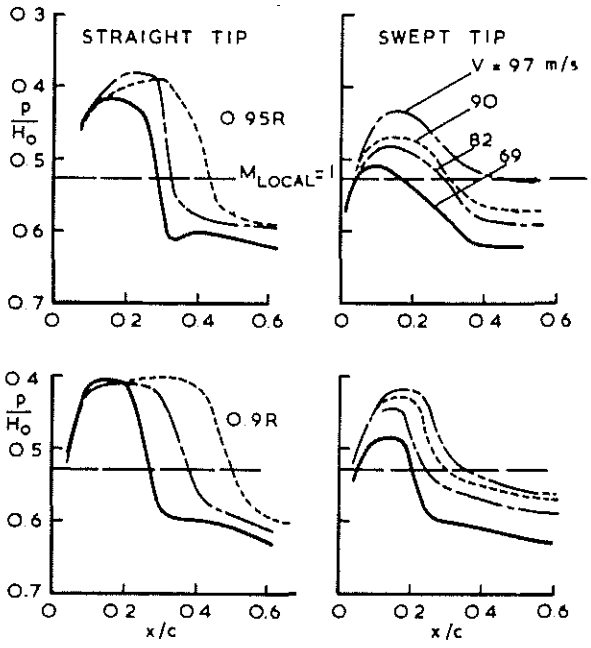

Fig 13 Measured pressure distributions at ψ = 90° for a range of forward speed

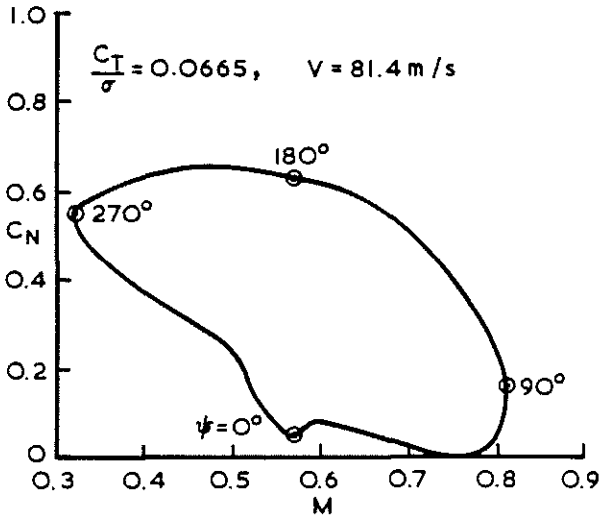

Fig 14 Operating conditions on model rotor with straight tip at 0.9R

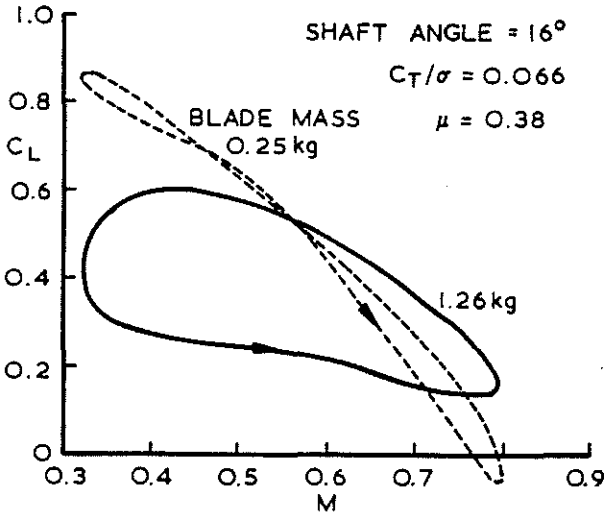

Fig 15 Predicted effect of blade mass on lift variation on straight tips at 0.9R in absence of cyclic pitch

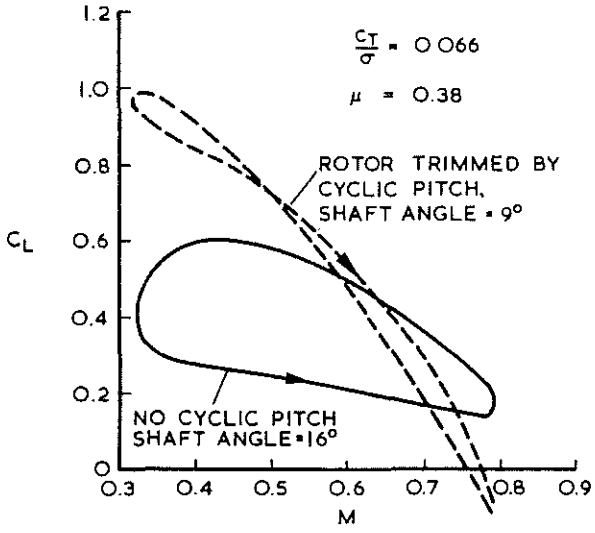

Fig 16 Predicted effect of cyclic pitch on lift variation at 0.9R for 'heavy' blades with straight tips

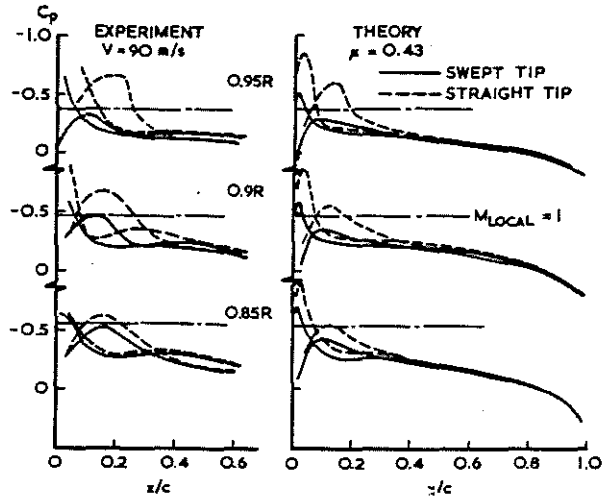

Fig 17 Comparison of experimental and theoretical pressure distributions at $\psi = 60^{\circ}$

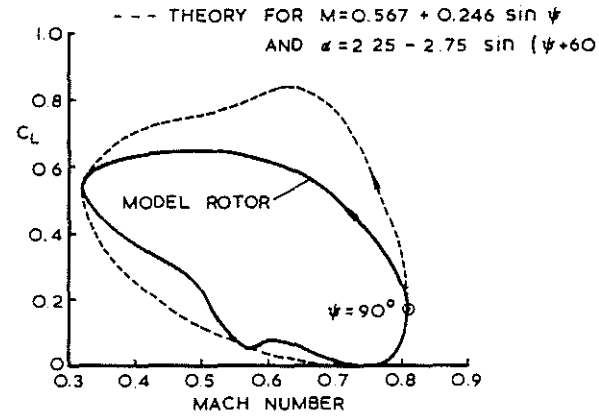

Fig 19 Two-dimensional simulation of conditions at 0.9R on rotor with straight tips

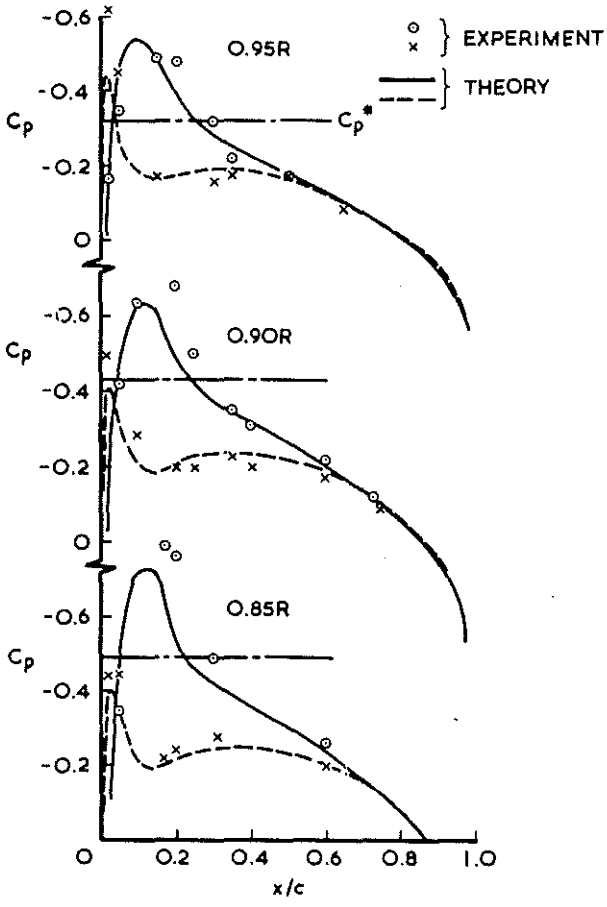

Fig 18 Comparison of experimental and theoretical pressure distributions at $\psi = 90^{\circ}$

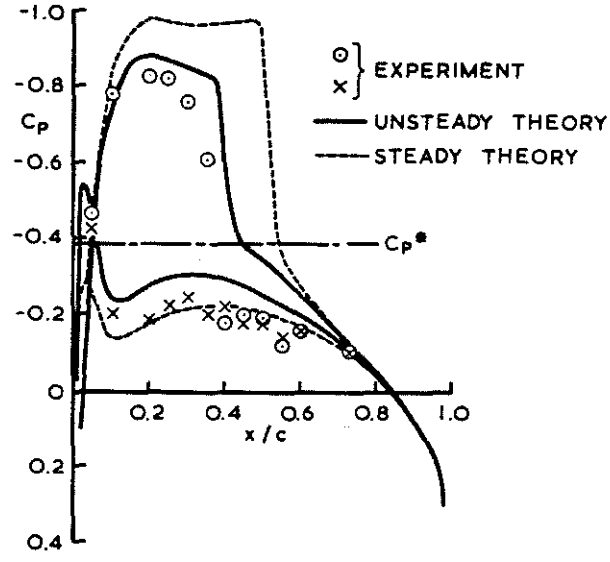

Fig 20 Comparison of measured pressure distribution on straight tip with two-dimensional theory